Fluorescence of Adsorbed Protein Layers. 1. Quantitation of Total Internal Reflection Fluorescence

ARTICLE *in* JOURNAL OF COLLOID AND INTERFACE SCIENCE · JUNE 1986

Impact Factor: 3.37 · DOI: 10.1016/0021-9797(86)90059-7

Fluorescence of Adsorbed Protein Layers

I. Quantitation of Total Internal Reflection Fluorescence

V. HLADY,[1] D. R. REINECKE,[2] AND J. D. ANDRADE[3]

Department of Bioengineering, College of Engineering, University of Utah, Salt Lake City, Utah 84112

Received October 9, 1985; accepted December 20, 1985

A quantitative total internal reflection intrinsic fluorescence (TIRIF) method for determining the adsorption of proteins at optically suitable solid/liquid interface is presented. Intrinsic protein fluorescence is excited by evanescent part of the standing wave produced by total internal reflection. The TIRIF data are quantified using as an internal standard the fluorescence from nonadsorbed proteins which are present in the evanescent region. In order to account for the fraction of fluorescence excited by scattered light which propagates through and beyond the volume sensed by the evanescent wave, a set of nonadsorbing external standards has to be used. The combination of TIRIF and ^{125}I–protein γ-photon detection system is described and applied to bovine serum albumin (BSA) and human immunoglobulin (IgG) adsorption at silica/electrolyte interfaces. The difference between the results obtained with different adsorption detection systems is discussed. An average fluorescence emission efficiency of adsorbed proteins can be evaluated by combining TIRIF adsorption data with the independent *in situ* quantitation of protein adsorption. It was found that in some cases adsorbed proteins emit fluorescence with significantly lower quantum yield.

INTRODUCTION

The concept of total internal reflection fluorescence (TIRF) at solid/liquid interfaces was introduced by Hirschfeld (1). Although this first use of TIRF was not applied to adsorbed species but to bulk dissolved dye, the advantage over the conventional fluorescence technique was demonstrated: fluorescence intensity vs concentration relation was linear up to a concentration 100-fold higher due to the shallow penetration of the evanescent wave. Applications of TIRF include collection of fluorescence from dansyl-bovine serum albumin molecules by TIRF optics (2), TIRF-based immunoassay for specific dye-labeled antibodies from the solution to an antigen coated surface (3), and "virometer," an optical sensor for viruses treated with a fluorescent probe bound to the virus nucleic acid (4, 5).

The applications of TIRF to the study of interactions between surfaces and proteins have been recently reviewed (6, 7). Two different routes to TIRF protein adsorption results are distinguished: in the first one the emission from those protein amino acids which intrinsically fluoresce upon excitation in ultraviolet, like tryptophan and tyrosine, is monitored; hence the name, total internal reflection *intrinsic* fluorescence (TIRIF), while in the second approach the emission from an *extrinsic* fluorophor covalently bound to the protein, such as fluorescein or rhodamine, is followed.

First approach parallels the protein solution fluorescence studies and allows one to analyze intrinsic protein fluorescence emission and excitation spectra, and other fluorescence phenomena. In principle, TIRIF can thus provide an insight to the conformational

[1] Presented at the 5th International Conference on Surface and Colloid Science, Clarkson University, Potsdam, N.Y., June 24–26, 1985, as part of a symposium entitled Protein and Polyelectrolyte Adsorption.

[2] This work was carried out when V. Hlady was on leave of absence from Institute "Ruđer Bošković," Zagreb, Yugoslavia.

[3] Taken in part from M.Sc. thesis of D. R. Reinecke, submitted to the University of Utah, July 1985.

[4] To whom correspondence should be addressed.

0021-9797/86 $3.00

changes in adsorbed proteins. It was shown recently that with appropriate apparatus based on total internal reflection, intrinsic fluorescence lifetimes of the adsorbed protein could be determined (8). Intrinsic fluorescence was also used in the TIRIF mode to study the adsorption of insulin, a protein molecule with a few tyrosine residues and no tryptophan in its structure (9).

The extrinsic fluor approach is more suitable to competitive protein adsorption studies and to protein adsorption kinetic studies, provided that the protein labeling by an extrinsic fluor does not cause different protein adsorbability. The uptake of fluorescein-labeled albumin, γ-globulin, and fibrinogen onto silicone rubber coated surfaces has been followed as a function of time (10). The adsorption of the same proteins was followed also as a function of flow rate of protein solution; it was demonstrated that adsorption is diffusion-limited (11). A combination of total internal reflection with fluorescence photobleaching recovery and fluorescence correlation spectroscopy was described and applied to the study of protein surface diffusion and exchange rates (12, 15).

In all TIRF protein adsorption experiments it is desirable to correlate the intensity of fluorescence with the excess protein concentration at the interface. The adsorbed layer is often in equilibrium with nonadsorbed protein molecules which are also situated inside the "evanescent volume" and contribute to overall fluorescence. Various methods have been proposed to calibrate TIRF data: (a) external nonadsorbing standards were used (13, 14); (b) some type of evanescent energy distribution calculation was preformed while solution proteins in the evanescent region were used as internal standards (14); and, (c) protein surface excess was measured independently (15).

However, inconsistent results often emerged and TIRF was considered to be only semiquantitative. It will be shown here that TIRIF can be made quantitative by using both external and internal fluorescence standards and by appropriate accounting for the part of fluorescence which is excited by scattered light propagating through and beyond the region sensed by the evanescent surface wave.

Quantitation Scheme of TIRIF

A full account of evanescent wave theory has been presented elsewhere (6, 14, 16). Only those parts pertinent to the present quantitation scheme will be given here. The TIRIF quantitation of protein adsorption is based on the distribution of evanescent electromagnetic radiation intensity beyond the reflecting solid/liquid interface. The superposition of incident and reflected waves in total internal reflection forms a standing wave in the optically more dense medium. The nature of the standing wave is a function of both the optically more dense medium (medium 1; here, a hydrophilic amorphous silica) and the less optically dense medium (medium 2; here, an aqueous protein solution). The electric field amplitude right at the interface in the denser medium has a nonzero value in the case of two dielectrics. Solution of Maxwell's wave equation for total internal reflection shows the existence of a surface wave which propagates along the interface (17). Since the boundary conditions for electromagnetic wave reflection do not allow any discontinuity of the tangential field across the interface, the electric field amplitude at the interface in medium 2 will be equal to the electric field amplitude at the interface in medium 1. The electric field amplitude of the evanescent wave, $E_{\perp}^{e}$, will decay exponentially with distance z normal to the interface in medium 2:

$$E_{\perp}^{e}(z) = (E_{\perp}^{t,0}/E_{\perp}^{i,0})\exp(-z/d_p)$$

$$= (2\cos\theta_1)/\{[1 - (n_2/n_1)^2]^{1/2}\} \times \exp(-z/d_p), \quad [1]$$

$$d_p = \lambda \cdot 1/[2\pi(n_1^2\sin^2\theta_1 - n_2^2)^{1/2}] \quad [2]$$

where $E_{\perp}^{t,0}$ is electric field amplitude right at the interface in less dense medium 2; $E_{\perp}^{i,0}$ is electric field amplitude of incident, perpendiculary polarized light; n_1 and n_2 are refractive

indices of the two media, θ_1 is the angle of incidence of electromagnetic wave measured from the interfacial normal, and d_p is defined as a distance from the interface where the electric field amplitude decrease to e^{-1} of its interfacial value. The parameter d_p is often called "depth of penetration of the evanescent wave." From the experimental point of view it is important to recognize that $[E_\perp^e(z)]^2$ is proportional to the profile of electromagnetic radiation intensity present in medium 2. Such profile determines the "surface sensitivity" of the particular evanescent wave.

In general, the observed fluorescence intensity is proportional to the product of incident light, and the probabilities of absorption and emission. When the evanescent region is populated with proteins, the fluorescence intensity N is given by

$$N = 2.303ab \int_0^\infty \Phi(z)[f(\lambda)](z) \times \epsilon(z)c(z)[E^e(z)]^2\, dz \quad [3]$$

where Φ is quantum yield. The extinction coefficient at excitation wavelengths ϵ, the protein concentration c, and the fraction of total fluorescence emitted at wavelength λ, $f(\lambda)$, are all given as a function of distance from the interface. The constant a accounts for the fraction of total fluorescence collected by the detector and $b \int [E^e(z)]^2\, dz$ is a term equivalent to the product of light path distance and incident light intensity, $d \cdot I_0$, in conventional spectrofluorometry (this makes $b = I_0 n_2 / 2.303 n_1 \cos\theta_1$). If the adsorbed protein layer has a thickness Δ, the ratio between the observed fluorescence intensities of adsorbed proteins N_a and nonadsorbed proteins N_b is given by

$$\frac{N_a}{N_b} = \frac{2.303ab \int_0^\Delta \Phi(z)[f(\lambda)](z)\epsilon(z)c(z)[E^e(z)]^2\, dz}{2.303ab \int_\Delta^\infty \Phi(z)[f(\lambda)](z)\epsilon(z)c(z)[E^e(z)]^2\, dz}. \quad [4]$$

Equation [4] can be simplified by assuming a step distribution of protein molecules in the evanescent region; for $0 < z < \Delta$ protein concentration c equals Γ_{vol}, and for $\Delta < z < d$, c equals c_p (d is thickness of TIRIF cell). It can be further assumed that ϵ, $f(\lambda)$, and $[E^e(z)]$ remain unchanged by the adsorption. Then

$$\frac{N_a}{N_b} = \frac{\Phi_a \Gamma_{vol} \int_0^\Delta [(E_\perp^{t,0}/E_\perp^{i,0})e^{-z/d_p}]^2\, dz}{\Phi_b c_p \int_\Delta^\infty [(E_\perp^{t,0}/E_\perp^{i,0})e^{-z/d_p}]^2\, dz}. \quad [5]$$

Figure 1a shows a typical TIRIF data output; introduction of protein into the TIRIF cell causes an increase of fluorescence intensity due to the protein adsorption. After a given period of protein interfacial residence time, nonadsorbed proteins in the cell are replaced with buffer solution and an immediate decrease of fluorescence intensity follows. Both N_a and N_b are thus experimentally accessible and Eq. [5] can be used to calculate Γ_{vol}. As a first approximation it can be assumed that the emission probability does not change by adsorption, i.e., that $\Phi_a/\Phi_b \approx 1$. The thickness of the adsorbed layer can be estimated from protein molecular dimensions. The implication of these assumptions will be discussed later.

Preliminary studies showed that the changes in fluorescence intensity after protein solution flush-out, N_b, varied considerably between repeated experiments, while N_a remained relatively constant. This indicated that beside the excitation by evanescent surface wave there was some other source of excitation which induced the fluorescence from nonadsorbed protein. It was found that the light scattered by imperfections in optical components of the TIRIF cell propagated through and beyond the evanescent region. Nonadsorbed protein molecules in the whole volume of TIRIF cell were excited by this scattered light and their fluo-

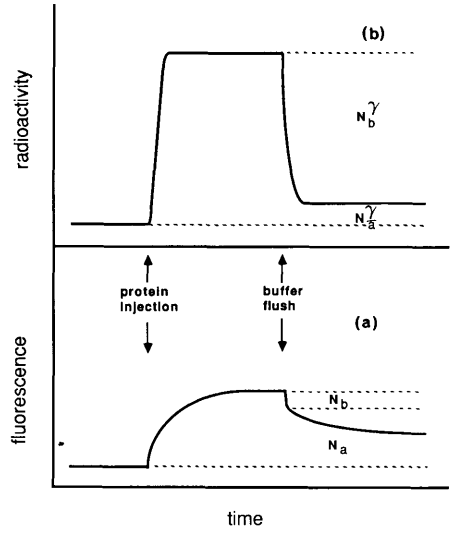

FIG. 1. An illustration of TIRIF data output (a) combined with the output of the parallel γ-photon detection (b) in a typical protein adsorption experiment. See text for explanation of symbols used.

rescence contributed to overall N_b signal. Different extent of scattering which varied from one optical interface to the other caused nonreproducible adsorption results. The same propagating nature of the scattered excitation light was used to correct N_b for its scatter-originated part. By increasing the concentration of a particular nonadsorbing standard which has the same fluorescence characteristics as the protein used (they will be referred to as external standard, subscripted by s), a condition can be attained at which the incident intensity of the propagated scattered excitation light is completely attenuated in the TIRIF cell volume, i.e., where $\epsilon_s c_s d > 2$. Since the fluorescence from the TIRIF cell is collected at the front face, any further increase of either d or c_s will not result in any further increase of fluorescence. The scatter-originated contribution to overall fluorescence will remain constant. On the contrary, fluorescence excited by the evanescent surface wave will, in this case, still increase linearly with increasing c_s due to the shallow penetration depth of the evanescent wave. The contributions of scatter-originated and evanescently excited fluorescence of nonadsorbing standards to overall fluorescence are given in Fig. 2. At the higher ϵc, the scatter-originated part becomes constant while the evanescently excited part increases linearly with concentration. The overall fluorescence intensity is the sum of both parts and depends on the thickness of TIRIF cell only at $\epsilon c < d/2$. The fluorescence excited by the evanescent surface wave can be resolved from the total fluorescence by translating the linear part of total fluorescence vs ϵc curve along the y axis until it passes through the origin. It represents the evanescent part of the total TIRIF signal, while the rest is the contribution excited by scattered propagating light. The ratio between the evanescent component N_s^e and the total fluorescence N_s^{tot} is unique for given ϵcd, wavelength of excitation, and experimental geometry. When the protein solution is in the TIRIF cell, it will absorb both the evanescent and the propagating excitation radiation in the same *relative* proportions as the external standards do at the same ϵc. Here, eventual rescattering of propagating light by protein molecules in the TIRIF cell is neglected. It is also assumed that the scattered propagating light in the TIRIF cell does not produce a significant fluorescence contribution from the adsorbed protein layer, since the thickness of this layer is much smaller than the TIRIF cell thickness.

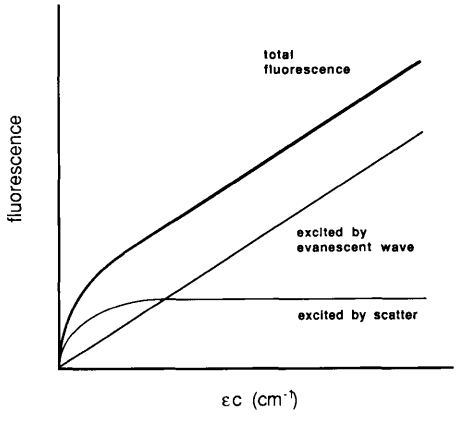

FIG. 2. Contributions of scatter-originated and evanescent wave excited fluorescence of nonadsorbed molecules to the total fluorescence collected from the TIRIF cell.

The absorbed radiation will be then reemitted as bulk protein fluorescence N_b^{tot} with an appropriate quantum yield. The evanescent part of N_b^{tot}, N_b^e, which should be used in Eq. [5] can be calculated as

$$N_b^e = N_b^{tot} \cdot N_s^e / N_s^{tot}|_{\epsilon cd=\text{const}}. \quad [6]$$

Note that N_b^{tot} is obtained in the presence of the adsorbed layer of thickness Δ, while the ratio N_s^e/N_s^{tot} is determined using the external standards in the absence of this layer. Due to this difference, N_b^e has to be corrected by a factor

$$\frac{\int_0^\infty [(E_\perp^{t,0}/E_\perp^{i,0}) \cdot e^{-z/d_p}]^2 \, dz}{\int_\Delta^\infty [(E_\perp^{t,0}/E_\perp^{i,0}) \cdot e^{-z/d_p}]^2 \, dz}$$

or Eq. [5] has to be rewritten as

$$\frac{N_a}{N_b^e} = \frac{\Phi_a \Gamma_{vol} \int_0^\Delta [(E_\perp^{t,0}/E_\perp^{i,0}) e^{-z/d_p}]^2 \, dz}{\Phi_b c_p \int_0^\infty [(E_\perp^{t,0}/E_\perp^{i,0}) e^{-z/d_p}]^2 \, dz} \quad [7]$$

which simplifies to

$$\frac{N_a}{N_b^e} = \frac{\Phi_a \Gamma_p}{\Phi_b c_p \Delta} (1 - e^{-2\Delta/d_p}) \quad [8]$$

where protein surface concentration Γ_p (mass/area) equals $\Gamma_p = \Delta \cdot \Gamma_{vol}$. Although the thickness of adsorbed protein layer is largely an unknown, it can be shown that the calculated amount of adsorbed protein Γ_p does not depend critically on the choice of Δ. As long as Δ is small, $(1 - e^{-2\Delta/d_p}) \approx 2\Delta/d_p$. Most protein dimensions are of the right order of magnitude. Furthermore, an average fluorescence quantum yield of adsorbed proteins can be evaluated by Eq. [8], provided that Γ_p is determined by an independent method, preferably *in situ*. Such information can provide an additional insight into the conformational changes of the adsorbed protein molecules.

EXPERIMENTAL

Materials

Fluorescence standard, 5-hydroxytryptophan methyl ester hydrochloride (TrpOH), was purchased from Calbiochem. Human immunoglobulin (IgG), fraction II (No. 64-145-1, lots 44 and 45) and bovine serum albumin (BSA) (monomer standard protein powder, No. 81-028, lot P341) were products of Miles Laboratories. Carrier free (100 mCi/ml) ^{125}I was purchased from New England Nuclear. Proteins were labeled with ^{125}I using a modified chloramine-T method (18) and separation procedure developed by Tuszinsky (19). Labeled proteins were stored at 4°C and used within 1 week. All solutions were made from analytical grade reagents and low conductivity water. All buffer solutions were tested for presence of fluorescence impurities. Both BSA and IgG were used without further purification. Unlabeled protein solution was prepared fresh prior to each experiment. Fluorescence of labeled and unlabeled proteins in solution was compared for evidence of ^{125}I-induced quenching. Protein stock solution concentration were determined using BSA and IgG extinction coefficients at 280 nm ($\epsilon_{BSA} = 0.667$, $\epsilon_{IgG} = 1.38$ liters $\cdot g^{-1} \cdot cm^{-1}$, respectively). Absorbances of internal and external standard solutions were always determined at particular excitation wavelengths prior to their use.

The hydrophilic amorphous silica microscope slides (ESCO Products) served as the adsorbing surfaces. Each surface for protein adsorption were cleaned as described earlier (20). The clean hydrophilic silica surface exhibited complete wetting and absence of contact angle hysteresis.

Methods

The TIRIF apparatus combined with γ-photon detection system has been described in details elsewhere (6, 21). The heart of this system was the dovetail quartz prism coupled with glycerol to the silica plate, as shown in Fig. 3. A Silastic (Dow Corning) gasket, at least 0.5 mm thick, formed a TIRIF flow field. Second silica plate with ports for solution injection was supported by a black-anodized aluminium support. The excitation source was a 150-W Xe high-pressure lamp. The excitation

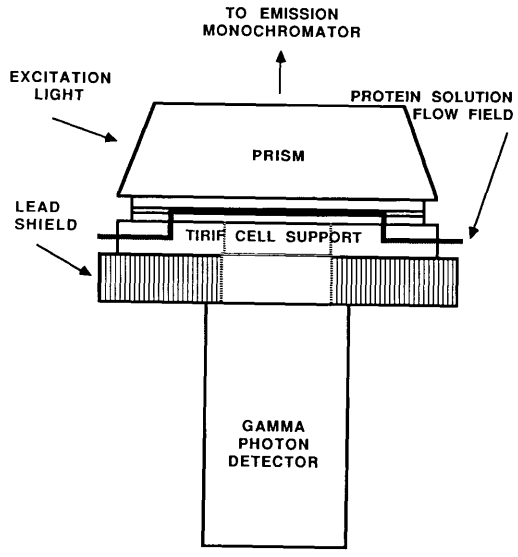

FIG. 3. Design of the TIRIF cell combined with γ-photon detector. The protein flow field is indicated.

monochromator with scan controller (H10-UV, Instrument, SA) was used to select the appropriate excitation wavelengths. A digital shutter, UV-polarizer and quartz optics delivered a perpendiculary polarized, collimated beam of UV light normal to the one face of the dovetail prism. Light impinged at the reflecting interface at the angle of 70°, exceeding the critical angle for total internal reflection at silica/water interface (θ_{crit} = 64.7°). Fluorescence was collected through the dovetail prism at normal incidence to the interface, focused on the slit of the emission monochromator (HR-640, Instrument SA, 300 gr/mm grating), and detected by a photomultiplier tube. Preamplified signals were counted by Ortec photon-counting equipment and recorded both in analog and digital form.

The γ-photon detection system consisted of NaI(Tl) scintillation crystal (2.5-cm diameter, 1.25-cm thick) joined to the face of second photomultiplier tube by a quartz light pipe, all enclosed in a light-tight steel jacket (custom designed, Bicron). A 2.5-cm-diameter sensing window covered by thin aluminum foil was situated directly behind the second silica plate with a circular detecting area defined by a lead shield. The signal from the second photomultiplier tube was preamplified and discriminated against a preset threshold before multiplexing with the TIRIF signal into the time-shared Ortec photon counting unit.

Quantitation of Protein Adsorption by γ-Photon Detection

A schematic of the γ-photon signals from a protein adsorption experiment is given in Fig. 1b. As in the case of TIRIF two distinct signal levels can be distinguished: N_a^γ and N_b^γ. Unlike TIRIF, γ-photon detection is not surface sensitive and detects γ-photon emission from the whole TIRIF volume. In the absence of preferential binding the detected signal was proportional to the mass of protein m in the sensing volume V (determined by radius r of the lead shield aperture and thickness of TIRIF cell, d):

$$N_b^\gamma = km_b; \quad m_b = c_p V = c_p \pi r^2 d, \qquad [9]$$

$$N_a^\gamma = km_a; \quad m_a = \Gamma_p^\gamma \cdot 2\pi r^2, \qquad [10]$$

and from N_b^γ and N_a^γ the adsorbed amount of protein can be calculated as

$$\Gamma_p^\gamma = (N_a^\gamma c_p d)/(2N_b^\gamma). \qquad [11]$$

Experimental Protocols

In situ TIRIF and γ-photon detected protein adsorption. All experiments were done at room temperature. For *in situ* protein adsorption experiments the TIRIF flow cell was primed with buffer solution after necessary optical alignments. Fluorescence emission was generated by exciting at 285 nm and collected at 335 nm (330 nm in the case of IgG adsorption). Slits of 16-nm half-bandwidth were used both in excitation and in emission monochromators. Background fluorescence and γ-photon counts were taken and buffer solution was replaced with the external standard (TrpOH) solutions in increasing order of concentration. The fluorescence intensity was recorded and between each standard sample the buffer solution was used to return the fluorescence signal to the background level. When both TIRIF

and γ-photon detection measurements were combined 3 ml of labeled protein solution were injected, the TIRIF cell was sealed and both signals were recorded. Adsorption was allowed to proceed for 30 min. The fluorescence counting time was 1 s for single measurements while the γ-photon counting system required at least 10 s of counting time. A digital shutter was used to prevent overexposure of adsorbed proteins to UV light. After 30 min, 20 ml of buffer solution was injected manually into the TIRIF cell to remove nonadsorbed proteins and both signals were recorded. The procedure was then repeated by injecting the next protein solution. An increasing order of protein concentration was used. In this way a step-adsorption experiment was performed as opposed to single-shot adsorption experiments where the clean silica surface was exposed only once to each protein solution. At the end of the adsorption experiment, a protein solution of the highest concentration used was injected into and flushed out of the TIRIF cell several times to obtain a reliable internal standard fluorescence signal.

Initial BSA adsorption kinetics were followed only by TIRIF; the cell was primed by 10 ml BSA solution at a flow rate of 16 ml/min after which the flow was stopped and the TIRIF cell sealed.

Ex situ protein adsorption on silica chips. Parallel to the *in situ* measurement of protein adsorption via the γ-photon detection system, similar *ex situ* measurements were performed using smaller rectangular chips of silica (total area of ≈ 5 cm^2) and a commercial γ-photon well counter. The experimental protocol simulated the *in situ* protocol, excluding the formation of any air-adsorbed protein interface. All *ex situ* and preferential binding experiments were performed in a single-shot manner. Details of *ex situ* measurements are given elsewhere (21).

Results

Fluorescence of external TIRIF standard. The fluorescence emission of TrpOH standard solutions (phosphate buffer, 0.145 *M* NaCl, pH 7.4) was centered at 340 nm. A typical background-subtracted fluorescence of external standards measured as a function of ϵc at different TIRIF cell thicknesses is shown in Fig. 4. The same silica plate was used while

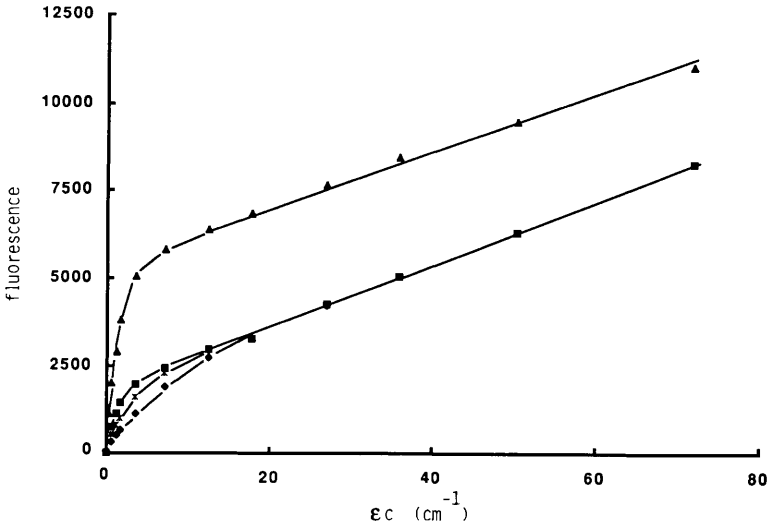

FIG. 4. Background subtracted fluorescence of (TrpOH) as a function of ϵc. Excitation at 285 nm, emission collected at 335 nm. TIRIF cell thickness: ♦, 0.7 mm; *, 1.4 mm; ■, 2.4 mm; ▲, 2.4 mm + silica dust mixed with optical matching fluid, glycerol.

cell thickness was increased from 0.7 to 1.4 and 2.4 mm, respectively (lower three curves). The upper curve was obtained with a 2.4-mm-thick TIRIF cell gasket after the scattering of the excitation light was greatly increased by mixing the optical matching fluid with crushed silica dust. In all four cases a linear increase of fluorescence was found at high ϵc. As one would expect, by reducing the cell thickness the linear part appears at higher values of ϵc. Before each protein adsorption experiment similar TrpOH calibration plot was generated for particular silica plate and cell gasket used. These plots were used in the quantitation procedure as previously described.

BSA adsorption on hydrophilic silica. The adsorption of BSA on hydrophilic silica from 0.01 *M* acetate buffer solutions of pH 4.8 and 4.0 was determined by the TIRIF and γ-photon (*in situ* and *ex situ*) detection system. The emission of BSA fluorescence is found to be centered at 342 nm (solution) and at 333 nm (adsorbed layer) at both pH. The fluorescence intensity of the internal BSA standard solution (0.5 mg/ml) was corrected for its scatter-originated part using the external (TrpOH) standard calibration plot determined in the beginning of the experiment. The TIRIF adsorption data were calculated using Eq. [8], assuming that $\Phi_a/\Phi_b = 1$. The thickness of the BSA layer was taken to be equal to 4 nm. The isotherms of BSA adsorption are combined in Figs. 5 and 6. One adsorption isotherm (Fig. 5, dashed line) was calculated from raw TIRIF fluorescence data without the external standard calibration plot. Preferential binding of ^{125}I–BSA molecules to the hydrophilic silica was not investigated.

Initial BSA adsorption kinetic from dilute protein solutions (c_p = 0.0193 mg/ml at pH 4.8, and c_p = 0.0259 mg/ml at pH 4.0, respectively), was followed on clean hydrophilic silica surfaces. At these low BSA concentrations the fluorescence contribution from nonadsorbed BSA was not significant. Moreover, diffusion of BSA to the surface was slow enough so that the process of the adsorption was followed in real time with TIRIF resolution of 1 s. The TIRIF adsorption kinetic data are given in Fig. 7 as a function of (time)$^{1/2}$. The diffusion-limited adsorption data for two BSA concentrations used (given as straight lines in Fig. 7) were calculated from Eq. [12]. They were shifted along x axis to match the start of the adsorption.

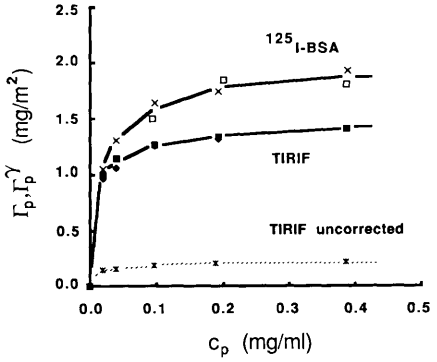

FIG. 5. TIRIF- and ^{125}I–BSA detected adsorption isotherms of BSA onto hydrophilic silica at room temperature, 0.01 M acetate buffer, pH 4.8. ♦, ■, TIRIF; □, ^{125}I–BSA *in situ* step-adsorption mode; ×, *ex situ* adsorption; *, TIRIF, uncorrected for scattering.

IgG adsorption on hydrophilic silica. Adsorption of IgG was followed from phosphate buffer solution (phosphate buffer, 0.145 *M* NaCl, pH 7.2). Preferential binding of ^{125}I–IgG to hydrophilic silica surface was investigated using IgG solutions of identical concentrations (0.18 mg/ml) which had different IgG radioactivities. The *in situ* γ-photon detection system was used. The results indicated that no preferential binding of ^{125}I–IgG has taken place. The fluorescence emission of IgG in the buffer solution was found to be centered at 340 nm. The adsorption of IgG on hydrophilic silica was measured by TIRIF and γ-photon detection (*in* and *ex situ*). The fluorescence of the internal IgG standard solution (0.8 mg/ml) was corrected for its scatter-originated part using an external (TrpOH) standard calibration plots. Both single-shot and step-adsorption experiments were performed. The results are summarized in Fig. 8. The TIRIF adsorption data have been calculated assuming that $\Phi_a/\Phi_b = 1$. The thickness of the IgG layer was

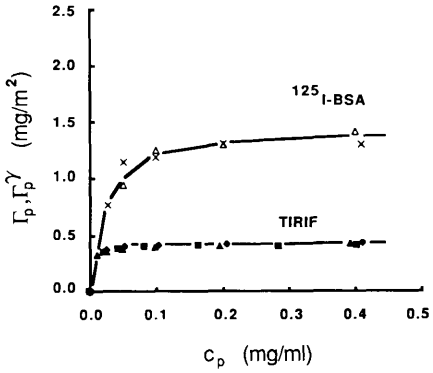

FIG. 6. TIRIF- and ^{125}I–BSA detected adsorption isotherms of BSA onto hydrophilic silica at room temperature, 0.01 *M* acetate buffer, pH 4.0. ♦, ■, ▲, TIRIF; △, ^{125}I–BSA *in situ* step-adsorption mode; ×, *ex situ* adsorption.

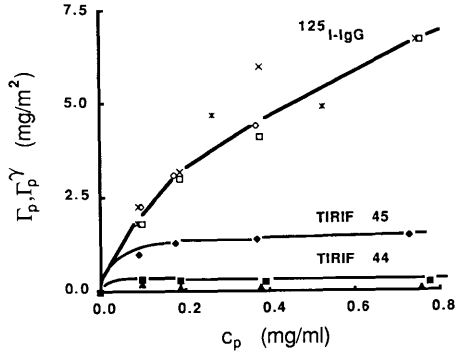

FIG. 8. TIRIF- and ^{125}I–IgG detected adsorption isotherms of IgG onto hydrophilic silica at room temperature, phosphate buffer, 0.145 *M* NaCl, pH 7.2. ♦, TIRIF, IgG lot 45; ▲, ■, TIRIF, IgG lot 45; ◇, □, ^{125}I–IgG *in situ* step-adsorption mode, lots 45 and 44, respectively; *, *in situ* single-shot adsorption mode; ×, *ex situ* adsorption.

assumed to be equal to 10 nm which roughly corresponds to the height of the "T"-shaped IgG molecule (22). Two TIRIF adsorption isotherms coded 44 and 45 represent two different IgG lots, respectively. No significant difference in the adsorption of two IgG lots was found in the case of γ-photon detected adsorption. Initial adsorption kinetics of IgG were not investigated.

Fluorescence emission efficiency of adsorbed proteins. In order to analyze the influence of adsorption on the fluorescence emission efficiency of BSA and IgG, the ratio of protein fluorescence quantum yields in the adsorbed layer and in the solution, Φ_a/Φ_b, was calculated. Equation [8] was used together with experimentally determined Γ_p^γ. The ratio Φ_a/Φ_b is given in Fig. 9 as a function of maximum adsorption fraction, $\Gamma_p^\gamma/\max \Gamma_p^\gamma$.

DISCUSSION

Most studies of protein adsorption by total internal reflection methods have focused on

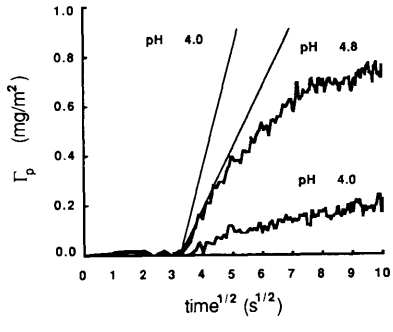

FIG. 7. Initial kinetics of BSA adsorption on hydrophilic silica at room temperature, 0.01 *M* acetate buffer. The straight lines represent diffusion limited rate of adsorption calculated from Eq. [12] for c_p = 0.0193 mg BSA/ml (pH 4.8) and 0.0259 mg BSA/ml (pH 4.0), respectively.

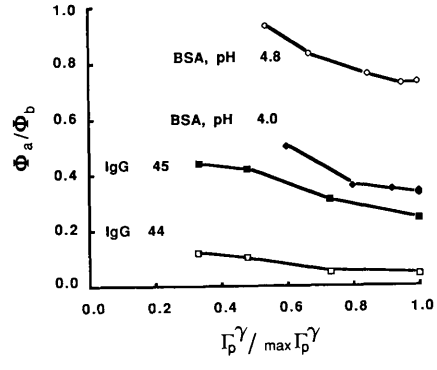

FIG. 9. The ratio of protein fluorescence quantum yields in the adsorbed layer and in the solution, Φ_a/Φ_b, given as a function of maximum adsorption fraction (as determined by γ-photon detection system), $\Gamma_p^\gamma/\max \Gamma_p^\gamma$.

the question: *how much* protein is adsorbed at a particular interface? To this end various quantitation schemes were proposed (13–15, 20). More often than not, they agreed that protein surface concentration had to be determined independently. Consequently, total internal reflection methods applied to protein adsorption were considered to be semiquantitative at best; the final adsorbed amount was determined by some independent method and all intermediate adsorption values were derived by scaling up or down measured fluorescence or absorbance in the case of attenuated total reflection methods. Such an approach was particularly successful in TIRF adsorption studies where proteins were labeled with an extrinsic fluorophore (10–13, 15).

The use of the fluorescence emitted by nonadsorbed proteins in solution as an internal standard in TIRIF experiments was initially proposed by Van Wagenen *et al.* (20). Later, Rockhold *et al.* proposed both graphical and numerical TIRIF quantitation schemes (14) but failed to recognize importance of scattered propagating excitation light. Present quantitation scheme is based on a similar concept; nonadsorbed proteins in the *evanescent* region are used as an internal fluorescence standard. However, in order to account fully for the extent of nonadsorbed bulk protein fluorescence excited by propagating scattered light, a number of external fluorescence standards of relatively large concentration range have to be used. It is also necessary to use such external standard whose excitation and emission characteristics are similar to the protein under study since the extent of scattering is related to $1/\lambda^4$ of excitation wavelength. As an external standard TrpOH was chosen; it has greater solubility than other tryptophan derivatives and its fluorescence emission is centered at 340 nm when excited at 285 nm.

The fluorescence from the standard solution should be dependent both on the TIRIF cell thickness and on the scattered light intensity due to the propagating nature of scattered light. Both effects were indeed found using solutions of TrpOH (Fig. 4). By increasing the thickness of the TIRIF cell the fluorescence intensity vs ϵc plots differed, but only at $\epsilon c < d/2$. This justifies the concept of calibration plots in TIRIF protein adsorption. From the experimental data at $\epsilon c < d/2$ it can be inferred that the scattered light in the TIRIF cell traveled a distance greater than the actual cell thickness. This was due to the wide range of angles at which the scattered light propagated in the TIRIF cell as well as due to the possible back-reflection from the second silica surface and TIRIF cell support.

Any rescattering of the excitation light by macromolecules in the TIRIF cell was examined by comparing the standard calibration plots of tryptophan (Trp) and tryptophan-labeled dextran (*N*-acetyl-tryptophanyl-dextran, $M_w = 70{,}000$). No significant increase of fluorescence was noticed; at given ϵc both Trp and Trp-dextran derivates fluoresced according to their respective quantum yields.

The TIRIF data of BSA adsorption on hydrophilic silica at pH 4.8 and the *in situ* and *ex situ* measured ^{125}I–BSA adsorption are of the same order of magnitude (Fig. 5). If the scatter-originated contribution to the fluorescence would be completely neglected, the TIRIF adsorption would amount to much lower values, as indicated by the adsorption isotherm given in dashed line (Fig. 5). By accounting for this part of the internal standard fluorescence sets the fluorescence-detected BSA adsorption is in reasonable agreement with both *in situ* and *ex situ* measured ^{125}I–BSA adsorption. However, the TIRIF adsorption experiments resulted in somewhat lower Γ_p which is particularly evident at higher BSA concentration. Possible reasons for this difference which may originate in some experimental artifacts or from the assumptions used, have to be considered in more detail.

Preferential binding of either ^{125}I-labeled or nonlabeled-BSA was ruled out since it was not detected in the case of BSA adsorption on a variety of surfaces (23). The fluorescence of ^{125}I-labeled and nonlabeled BSA in solution

was identical, with no evidence of ^{125}I-induced quenching.

The BSA molecules in the adsorbed layer may themself become scattering sources for the evanescent surface wave, which would induce a larger N_b. Since the calibration plots were generated with the external standards in the absence of adsorbed layers, this effect will result in smaller Γ_p. Use of the external standards with the adsorbed protein layer in place was not possible. The 285-nm excitation peak intensity in the fluorescence emission spectra which were taken prior to and after the BSA adsorption was not significantly increased. The question is whether this peak fully reflects the extent of scattering in the TIRIF cell? No scattering of the evanescent wave by adsorbed cells at glass/water interface was detected (7), although the scattering of the evanescent wave is predicted and analyzed in electromagnetic theory (24).

Second possible reason for the adsorption isotherm difference may be due to the different refractive indices of the protein solution and the adsorbed protein layer. There is little doubt that such difference exists; a 30% BSA solution has a refractive index of 1.41 at 285 nm (25), as compared with the dilute protein solution where the refractive index was taken to be equal to that of buffer solution (n_2 = 1.353). The quantitation scheme used here does not recognize the adsorbed proteins as a separate optical layer. The influence of an increased refractive index of adsorbed protein layer on electromagnetic energy distribution in the evanescent region is, however, smaller than intuitively expected. Due to the continuity requirement of the electric field amplitudes at the interface, any increase of $E_\perp^e$ in the part of evanescent region occupied by adsorbed protein will be followed by an increased $E_\perp^e$ outside the adsorbed layer. Hence, the ratio of integrals in Eq. [5] will not significantly change in value. For example, an increase of refractive index of the adsorbed layer from 1.353 (n_2 of aqueous phase) to 1.496 (n_1 of silica) will change the ratio of integrated evanescent intensities by a factor of 0.95. This would result as 5% higher adsorption! Hence, these two effects just compensate each other.

The most probable reason for the adsorption isotherm differences is a decreased fluorescence quantum yield of the adsorbed BSA molecules. Namely, the adsorption of protein at the interface may result in fluorescence surface quenching and shorter fluorescence lifetimes. It is also expected that a degree of protein unfolding at the interface could decrease the fluorescence emission efficiency.

The difference between two types of BSA adsorption isotherms is much larger at pH 4.0 (Fig. 6). Repeated TIRIF experiments on different silica plates showed excellent reproducibility of the adsorption results (Fig. 6). Yet, the BSA surface concentration detected by γ-photon detection was almost 3 times larger even when the scatter-originated fluorescence contribution was taken into account. No evidence of significantly increased scattering by the adsorbed BSA layer at pH 4.0, as compared with pH 4.8, was found. Also, no increase of refractive index of adsorbed BSA layer could possibly account for this large difference in the adsorption. Hence, the difference is largely determined by a decreased fluorescence efficiency of the adsorbed BSA molecules at the interface.

It is plausible that at its isoelectric point (pH_{iep} 4.8) BSA molecule does not experience the same conformational changes during the adsorption as it does when the adsorption is carried out from the more acidic solutions. The decrease of BSA quantum yield in acidic solution in which BSA molecule undergoes so-called "N–F transition" is well documented (26). However, this decrease has already been taken into the account in the present quantitation scheme by using BSA solution of pH 4.0 as the internal standard. At pH 4.0 BSA molecules are positively charged, while silica surface carries the negative charges. The attraction forces between opposite charges can contribute to BSA unfolding, if any, at the interface; this may induce a decreased fluores-

cence efficiency. Recently, similar conclusion has been reached from the TIRIF lifetime measurements of intrinsic BSA fluorescence from the adsorbed layer (8). The fluorescence lifetimes of adsorbed BSA molecules were found to be shorter than the lifetimes in solution.

The initial kinetics of BSA adsorption supports the conclusion about decreased fluorescence quantum yields. At pH 4.8 there is a good agreement between the initial TIRIF adsorption vs $(\text{time})^{1/2}$ data and the adsorption data calculated from the diffusion-limited rate of arrival of BSA molecules to the surface (Fig. 7). The latter rate, often called "diffusion-limited rate of adsorption," was calculated using (23)

$$d\Gamma_p = 2c_p(D/\pi)^{1/2}\, dt^{1/2} \qquad [12]$$

where D is BSA diffusion coefficient (7×10^{-7} $cm^2\ sec^{-1}$) (27). The coincidence between the initial TIRIF adsorption data and the calculated diffusion-limited adsorption indicates that at the beginning of the adsorption, $\Phi_a/\Phi_b = 1$. In the case of BSA adsorption at pH 4.0 the diffusion-limited adsorption exceeded TIRIF adsorption data. Similar difference between the experimental adsorption data and the diffusion-limited adsorption was found in BSA adsorption on glass and negatively charged polystyrene surfaces. It was explained by an energy barrier of adsorption (23). Namely, not all BSA molecules diffusing to the surface are "ready" to become adsorbed; only those with enough energy needed to overcome the adsorption energy barrier will "stick" to the surface.

Initial adsorption kinetics could not be followed with the *in situ* γ-photon detection system. This was due to low time resolution and relatively high bulk BSA contribution to overall γ-signal even at low BSA concentration. The following analysis could be done: TIRIF-detected adsorption at pH 4.0 was proportionally increased using as a reference point the final surface concentration of ^{125}I–BSA, Γ_p^γ, at the same c_p. In this way TIRIF adsorption data were corrected for the quantum yield decrease. They were compared with calculated diffusion-limited adsorption rate. The latter was still exceeding the experimental rate by a factor of 0.3. Such an adsorption rate decrease by a factor of $e^{-A/kT}$ would be due to an adsorption energy barrier A of $1.2kT$ units.

Interestingly, initial BSA adsorption at pH 4.0 reveals that the first contact between the protein and the silica surface immediately results in decreased fluorescence emission efficiency. It indicates that some conformational changes are taking place at very short interfacial residence times and at very low surface coverages. The picture is different at pH 4.8; the TIRIF adsorption data deviate from the diffusion limited adsorption data only at $\Gamma_p > 0.4$ mg m^{-2}. This may also be due to the limitation of Eq. [12] which is derived using the assumption that the surface acts as a protein sink. When there is more protein accommodated on the surface, however, less chance a new diffusing BSA molecule has to find an unoccupied adsorption site and adsorption slows down.

Possible conformational changes due to the adsorption are best illustrated by the ratio of protein fluorescence quantum yields in the adsorbed layer and in the solution, Φ_a/Φ_b, which is given in Fig. 9. It amounted to an average of 0.9 at pH 4.8 and to 0.5 at pH 4.0, respectively, as measured at the half maximum adsorption (at $\Gamma_p^\gamma/\max \Gamma_p^\gamma = 0.5$). Unfortunately, there is no direct relation between a degree of conformational BSA change and decreased fluorescence efficiency. The intrinsic fluorophors in proteins report their environment seen at the time of the emission. The BSA fluorescence is largely determined by two tryptophan residues although the energy available to their emission can be transferred to them from several tyrosines residues along the polypeptide chain. Overall photophysical "sensitivity" of BSA fluorophors to the conformational alterations in various parts of BSA molecule is not yet known. Before this information is available, a decrease of Φ_a/Φ_b at pH

4.0 may only serve as an indication that adsorbed BSA is conformationally changed.

The situation is even less clear in the case of IgG adsorption. Different isotherms of IgG adsorption on hydrophilic silica from phosphate buffer were determined depending on the method of detection used; TIRIF-detected adsorption depended on the particular IgG lot used, while ^{125}I–IgG-detected adsorption was almost independent on IgG lot used but it was an order of magnitude larger (Fig. 8). No difference between the fluorescence quantum yields of two different IgG lots could be detected in solution. Preferential adsorption of ^{125}I-labeled or unlabeled IgG on hydrophilic silica was excluded. Also, there was no evidence of ^{125}I-induced quenching of IgG fluorescence in the solution. It may be concluded that the labeling of IgG was not the cause of difference between the TIRIF and ^{125}I-labeled IgG adsorption isotherms.

The extent of scattering due to IgG molecules at the interface was considerably larger than in the case of BSA; the excitation peak maximum increased approx 30% for both lots. Increased intensity of scattered excitation light was also evident in the fluorescence of nonadsorbed IgG molecules in TIRIF cell. It was compared with TrpOH standards at given ϵc. The ratio of TrpOH/nonadsorbed IgG fluorescence intensities decreased as the surface concentration of IgG increased in the step-adsorption experiments. The fluorescence quantum yield of nonadsorbed IgG molecules in the TIRIF cell should not depend on the adsorption. Since the depletion of IgG was excluded an alternative explanation was that the intensity of excitation light increased due to the adsorption. Such an increase was estimated to amount up to 45%; it would decrease TIRIF adsorption results in the same proportions.

Two other factors may also influence the TIRIF-detected adsorption; a larger thickness of the adsorbed IgG layer and/or an increase of its refractive index. The influence of adsorbed layer thickness can be estimated: at constant Γ_p, an increase of Δ from 10 to 20 nm alone would increase calculated adsorption by 10%. Similar result would be found if the difference between the refractive indices was taken into the account. Again, all these effects compensate each other. Therefore, such a large difference between two types of the adsorption results may only originate in significantly decreased fluorescence efficiency of IgG molecules in the adsorbed state.

Not all tryptophan side chains contribute equally to IgG fluorescence; predominant contributors are tryptophans in hypervariable region (28). Because of that, ligand-binding to IgG often results in a decrease of fluorescence. In the present case IgG fluorescence may be quenched upon the binding to the surface. The surface-induced fluorescence quenching is currently studied by TIRIF using monoclonal IgG antibodies. The intrinsic IgG fluorescence is found to be a sensitive indication of subtle changes in this protein upon binding to various surfaces (29). An increased interest in TIRF-based immunosensors warrants further research in this area (29–31).

Difference between the two types of IgG adsorption detection is also reflected in the ratio of protein fluorescence quantum yields, Φ_a/Φ_b, given in Fig. 9. The fluorescence efficiency of adsorbed IgG has apparently decreased by a factor of 3 and 10 for lots 45 and 44, respectively. Both IgG lots were heterogenous populations of proteins commonly defined as fraction II. It is therefore possible that an IgG subpopulation with a higher affinity toward silica surface is also characterized with a smaller quantum yield of fluorescence.

It has to be noted that decreased fluorescence quantum yield of adsorbed proteins also reflects some possible changes of adsorption parameters, particularly of ϵ, which were assumed not to change upon the adsorption. The extents of change of ϵ are unknown. One would, however, expect that in the case of multitryptophan proteins such as IgG, the changes of ϵ due to the adsorption would be too small to account for observed difference.

Figure 9 shows that Φ_a/Φ_b decreases as

$\Gamma_p^\gamma/\max \Gamma_p^\gamma$ increases. Possible reasons for this were already discussed: (a) an increase of scattering due to the formation of an adsorbed layer at the interface; (b) the adsorbed protein layer may become physically different, i.e., thicker and optically more dense as the adsorption proceeds; and also (c) lateral interactions may also play an important role in determining the fluorescence emission efficiency of adsorbed proteins.

The optical changes of adsorbed protein layer were recently confirmed by ellipsometric measurements (32, 33).

CONCLUSION

It has been shown that total internal reflection fluorescence applied to protein adsorption can be quantitated using two types of standards; with external standards one can account for the fluorescence of internal standards excited by nonevanescent scattered radiation propagating beyond the depth of evanescent wave penetration. We believe that this quantitation scheme is neither restricted to *intrinsic* protein fluorescence nor to the TIRIF method in particular. It can be applied to adsorption studies which generally use evanescent surface wave. Combined with an independent quantitation of protein adsorption, quantitative TIRIF also allows an average fluorescence emission efficiency of adsorbed proteins to be calculated. To do so *in situ* ^{125}I γ-photon detection system was developed. The adsorption of two model proteins, BSA and IgG, were measured simultaneously by both TIRIF and ^{125}I γ-photon detection. The results showed that the assumption of a constant fluorescence quantum yield of proteins in the adsorbed layer and in the bulk solution should be used with caution. While for BSA at iep relatively small difference between the quantum yields was determined, much larger difference seen at IgG adsorption, and in the case of BSA adsorption at pH 4.0, could only be explained by a greatly diminished fluorescence efficiency.

ACKNOWLEDGMENTS

Discussions with P. Suci, W. M. Reichert, and R. A. Van Wagenen are gratefully acknowledged. The assistance from H. Chuang with protein iodination is appreciated. One of us (V.H.) acknowledges with appreciation a Fulbright Program Grant awarded for academic year 83/84. Part of this work was supported by financial help from a University of Utah Faculty Research Grant and NIH Grant HL 18519.

REFERENCES

1. Hirschfeld, T., *Canad. Spectrosc.* **10,** 128 (1965).
2. Harrick, N. J., and Loeb, G. I., *Anal. Chem.* **45,** 687 (1975).
3. Kronick, M. N., and Little, W. A., *J. Immunol. Meth.* **8,** 235 (1975).
4. Hirschfeld, T., and Block, M. J., *Opt. Eng.* **16,** 406 (1977).
5. Hirschfeld, T., Block, M. J., and Mueller, W., *J. Histochem. Cytochem.* **25,** 719 (1977).
6. Hlady, V., Van Wagenen, R. A., and Andrade, J. D., *in* "Surface and Interfacial Aspects of Biomedical Polymers, Vol. 2. Protein Adsorption" (J. D. Andrade, Ed.), Chap. 2. Plenum, New York, 1985.
7. Axelrod, D., Burghardt, T. P., and Thompson, N. L., *Ann. Rev. Biophys. Bioeng.* **13,** 247 (1984).
8. Rainbow, M. R., Atherton, S., and Eberhard, R. C., *J. Biomed. Mater. Res.*, submitted, 1985.
9. Iwamoto, G. K., Van Wagenen, R. A., and Andrade, J. D., *J. Colloid Interface Sci.* **86,** 581 (1984).
10. Watkins, R. W., and Robertson, C. R., *J. Biomed. Mater. Res.* **11,** 915 (1977).
11. Lok, B. K., Cheng, Y.-L., and Robertson, C. R., *J. Colloid Interface Sci.* **91,** 104 (1983).
12. Thompson, N. L., and Axelrod, D., *Biophys. J.* **43,** 103 (1983).
13. Lok, B. K., Cheng, Y.-L., and Robertson, C. R., *J. Colloid Interface Sci.* **91,** 87 (1983).
14. Rockhold, S. A., Quinn, R. D., Van Wagenen, R. A., Andrade, J. D., and Reichert, W. M., *J. Electroanal. Chem.* **150,** 261 (1983).
15. Burghardt, T. P., and Axelrod, D., *Biophys. J.* **33,** 455 (1981).
16. Hansen, W. N., *Advan. Electrochem. Electrochem. Eng.* **9,** 1 (1973).
17. Born, M., and Wolf, E., "Principles of Optics," 5th ed., Pergamon, New York, 1975.
18. Chuang, H. Y. K., King, W. F., and Mason, R. G., *J. Lab. Clin. Med.* **92,** 483 (1978).
19. Tuszynski, G. P., Knight, L., Piperno, J. R., and Walsh, P. N., *Anal. Biochem.* **106,** 118 (1980).
20. Van Wagenen, R. A., Rockhold, S. A., and Andrade, J. D., *Advan. Chem. Ser.* **199,** 351 (1982).
21. Reinecke, D. R., M.Sc. thesis, Univ. of Utah, 1985.

22. Bagchi, P., and Birnbaum, S. M., *J. Colloid Interface Sci.* **83,** 460 (1981).
23. Van Dulm, P., and Norde, W., *J. Colloid Interface Sci.* **91,** 248 (1983).
24. Chew, H., Wang, D.-S., and Kerker, M., *Appl. Opt.* **18,** 2679 (1979).
25. Andersen, M., and Painter, L. R., *Biopolymer* **13,** 1261 (1974).
26. Sogami, M., Itoh, K. B., and Nemoto, Y., *Biochim. Biophys. Acta* **393,** 446 (1975).
27. Keller, K. H., Canales, E. R., and Yum, S. I., *J. Phys. Chem.* **75,** 379 (1971).
28. Schreiber, A. D., Strosberg, A. D., and Pecht, I., *Immunochemistry* **15,** 207 (1978).
29. Lin, J-N., Hlady, V., Reichert, W. M., and Andrade, J. D., to be published.
30. Newby, K., Andrade, J. D., Benner, R. E., and Reichert, W. M., *J. Colloid Interface Sci.* **111,** 000 (1986).
31. Sutherland, R. M., Dähne, C., Place, J. F., and Ringose, A. R., *J. Immunol. Meth.* **74,** 253 (1984).
32. Cuypers, P. A., Corsel, J. W., Janssen, M. P., Kop, J. M. M., Hermens, W. Th., and Hemker, H. C., *J. Biol. Chem.* **258,** 2426 (1983).
33. Cuypers, P. A., Corsel, J. W., Janssen, M. P., Kop, J. M. M., Hermens, W. Th., and Hemker, H. C., *in* "Surfactants in Solution" (K. L. Mittal and B. Lindman, Eds.), Vol. 2, p. 1301. Plenum, New York, 1984.